ORIGINAL ARTICLE

Predictive modelling and latent space exploration of steel profile overstrength factors using multi-head autoencoder-regressors

Michael A. Kraus[1] | Andreas Müller[2] | Rafael Bischof[3] | Andreas Taras[2]

Correspondence

Dr. Michael A. Kraus
ETH Zurich
Institute of Structural Engineering
Stefano-Franscini-Platz 5
8093 Zurich / Switzerland
Email: kraus@ibk.baug.ethz.ch

[1] ETH Zurich, Concrete Structures and Bridge Design & Design++, Zurich, Switzerland
[2] ETH Zurich, Steel and Composite Structures & Design++, Zurich, Switzerland
[3] Swiss Data Science Center

Abstract

This paper investigates the suitability and interpretability of a data-driven deep learning algorithm for multi cross sectional overstrength factor prediction. For this purpose, we first compile datasets consisting of experiments from literature on the overstrength factor of circular, rectangular and square hollow sections as well as I- and H-sections. We then propose a novel multi-head encoder architecture consisting of three input heads (one head per section type represented by respective features), a shared embedding layer as well as a subsequent regression tail for predicting the overstrength factor. By construction, this multi-head architecture simultaneously allows for (i) the exploration of the nonlinear embedding of different cross-sectional profiles towards the overstrength factor within the shared layer, and (ii) a forward prediction of the overstrength factor given profile features. Our framework enables for the first time an exploration of cross-section similarity w.r.t. the overstrength factor across multiple sections and hence provides new domain insights in bearing capacities of steel cross-sections, a much wider data exploration, since the encoder-regressor can serve as meta model predictor. We demonstrate the quality of the predictive capabilities of the model and gain new insights of the latent space of different steel sections w.r.t. the overstrength factor. Our proposed method can easily be transferred to other multi-input problems of Scientific Machine Learning.

Keywords

Overstrength Factor, Scientific Machine and Deep Learning, Encoder-Regressor

1 Introduction

The nonlinear performance of steel structures is significantly influenced by the flexural behaviour of their load-bearing components. For reliable and robust design, the ability of members of a steel construction to provide adequate local ductility for developing plastic hinges without losing their moment capacity and thus ensuring redistribution of bending moments is critical for a global dissipative mechanism. For the bending of steel beams, the two governing parameters rotation capacity r and flexural overstrength s [1] are decisive, cf. Fig. 1. It is know, that r characterises beam ductility for achieving global dissipative structural behaviour while the flexural overstrength (the ratio of the maximum bending moment to the plastic bending moment) of steel beams s must be accurately known when applying capacity design principles recommended by modern seismic codes such as EN 1998.

Plastic deformation of ductile beams is characterized by an amount of strain hardening, responsible for the development of bending moments larger than the plastic bending strength. Therefore, it is essential to quantify the maximum bending moment experienced by the beams to design non-dissipative elements such as connections and columns. To ensure safe and efficient performance of steel structures during seismic events, designers must consider the flexural behaviour of steel beams in their designs. However current seismic codes provide design rules underestimating the actual ultimate flexural strength of steel beams due to the absence of mathematically correct formulas covering geometric and mechanical aspects over different cross section types.

Empirical methods have been proposed to estimate r and s of steel members using experimental and/or numerical data. However, there is a lack of comprehensive analytical estimation thereof for circular (CHS), rectangular (RHS) and square (SHS) hollow sections, as well as I and H profiles. This study aims to create a precise and efficient deep learning technique for forecasting the flexural overstrength factor of steel beams with varying cross sections under pure bending. This method enables identification and interpretation of latent correlations and provides a better understanding of cross-sectional similarities w.r.t s.

2 The Flexural Overstrength Factor *s*

The flexural overstrength factor *s* is a non-dimensional parameter used for characterizing the ultimate bending capacity of steel beams exceeding the plastic bending strength due to the strain hardening [2]. It is originally ([3],[4]) computed by the ratio of the stress f_{LB} corresponding to complete local buckling development or the lateral torsional buckling to the yield stress f_y

$$s = \frac{f_{LB}}{f_y} = \frac{M_u}{M_p} \qquad (1)$$

or by the more practical relation using the maximum moment M_u to the theoretical full plastic moment M_p. The ultimate bearing capacity of steel beams can be significantly greater than the plastic bending strength because of strain hardening before complete local buckling or fractures as given in Figure 1 by the generalized moment-rotation curves. The overstrength factor is used for seismic design in the Italian codes OPCM 3274 (2003) and NTC 2018 but neglected for cross-section classes in Eurocode 3 (EN 1993:1-1).

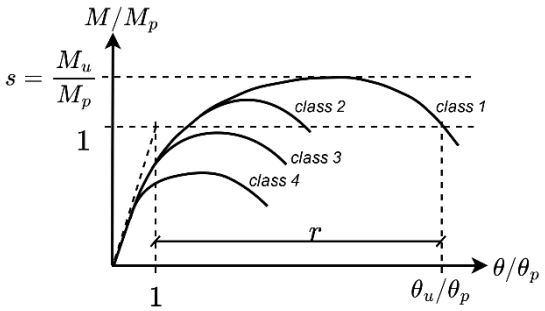

Figure 1 Generalized moment–rotation curve for a steel beam and EN 1993:1-1 classification criteria, (both after [2]).

3 Database Compilation and Properties

The databases used for calibrating our deep learning model for predicting the flexural overstrength factor *s* for CHS, RHS, SHS and I-H steel beams were collected from the available scientific literature [2], [5]-[27], [36]- [38].

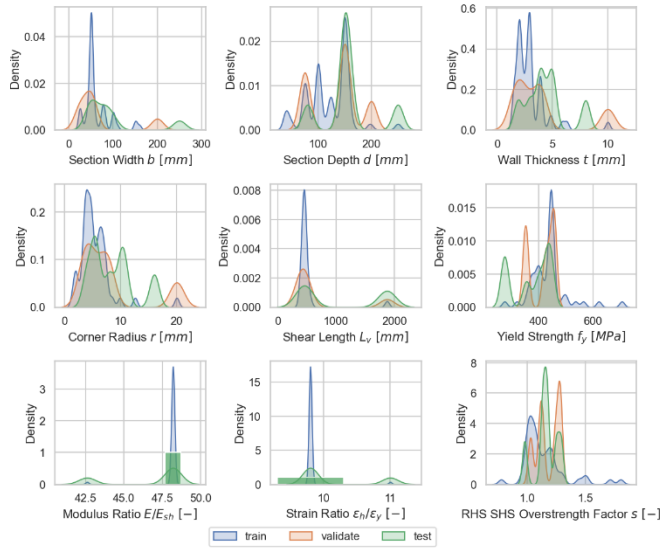

Figure 2 Probability densities of features and target of the RHS / SHS cross sections for the train, validation and test set.

The examined test configurations accounting for different load patterns (i.e. bending moment distribution) and cross-sectional. Figs. 2 – 4 proof the databases to contain samples covering a wide range of cross-sectional typologies under monotonic loading with different local slenderness ratios. The features consist of geometric properties of the section, mechanical properties of the material, and the shear length of the steel beams.

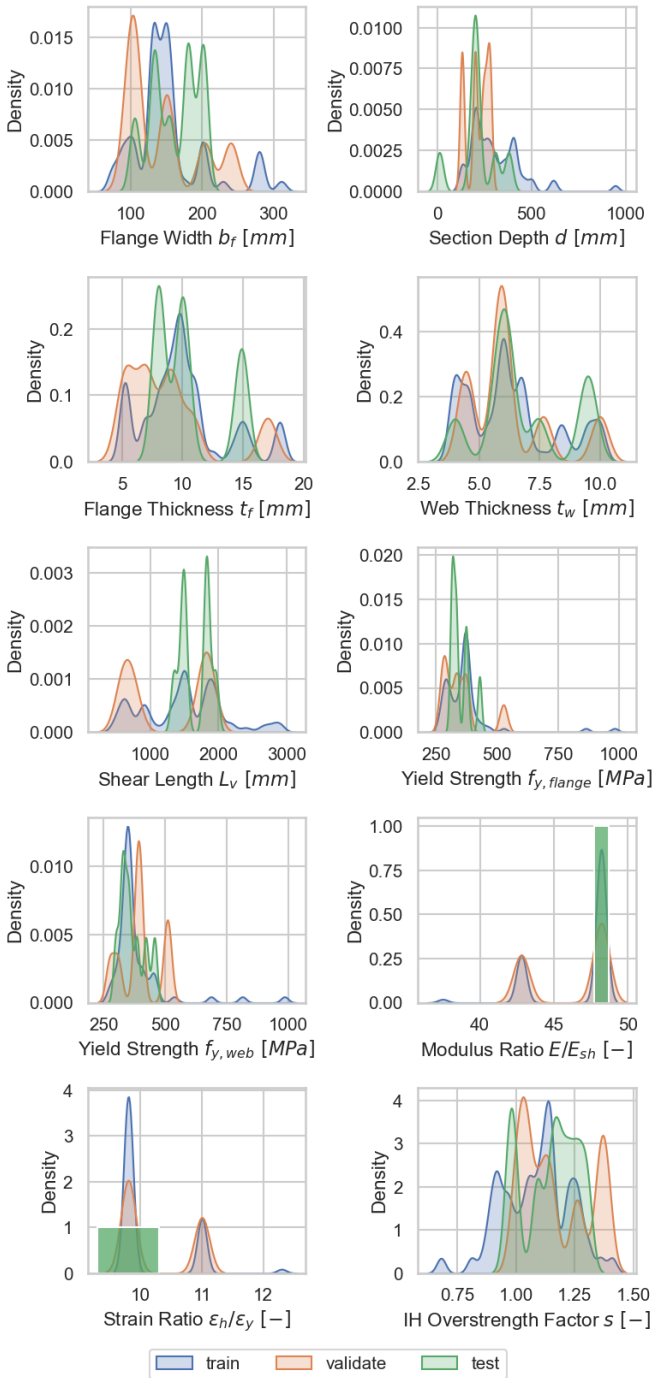

Figure 3 Probability densities of features and target of the I / H cross sections for the train, validation and test set.

The data set for ***circular* sections** contains 128 samples with features: section diameter *D*, thickness *t*, shear length *Lv*, yield strength *fy*. The data set for ***I-H* sections** consists of 76 samples with features: flange width b_f, section depth *d*, flange thickness t_f, web thickness t_w, shear length L_v, flange yield stress $f_{y,\text{flange}}$, web yield stress $f_{y,web}$, ratio of the modulus of elasticity of steel to the hardening modulus E/E_h, and ratio of the strain corresponding to the

beginning of hardening to the yield strain $\varepsilon_h/\varepsilon_y$. The data set for **RHS-SHS sections** comprises of 76 samples with features : section width b, section depth d, wall thickness t, inside corner radius r, shear length Lv, yield stress f_y, modulus ratio E/E_h, and strain ratio $\varepsilon_h/\varepsilon_y$.

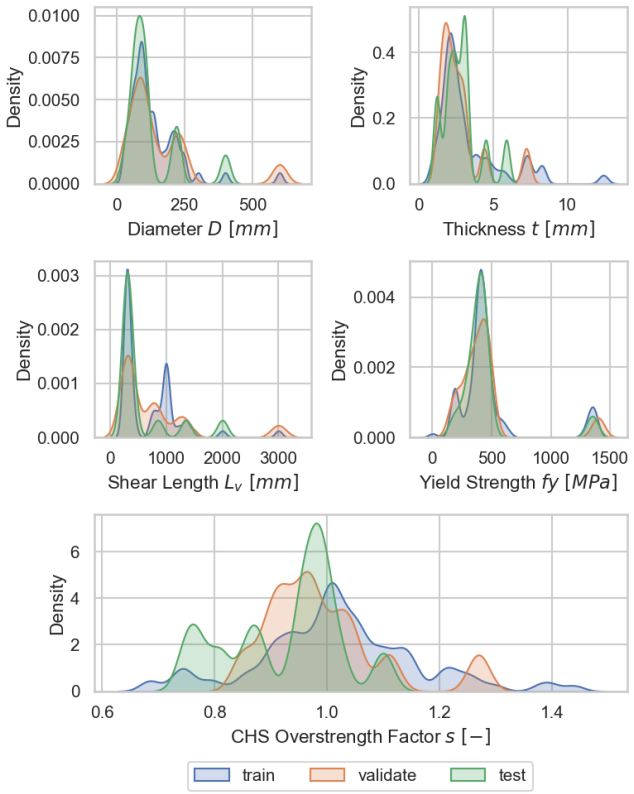

Figure 4 Probability densities of features and target of the CHS sections for the train, validation and test set.

4 Deep Learning Methods

4.1 State of the Art of DL in Structural Engineering and Computational Mechanics

Machine Learning (ML) and Deep Learning (DL) have been applied to the analysis and design of structural systems since 1989 [29]. Since then, these methods have been used for various other applications in the construction industry, as summarized in [30]. Recent developments in Artificial Intelligence (AI) at the interface of natural and engineering sciences have led to the formation of the terms "physics-informed" and "domain-informed" AI [31]. Applications of these concepts, as well as additional backgrounds and examples, can be found in [32] for constructive glass design, [31, 36-42] for steel design, and [34,35] for concrete and bridge design.

This paper specifically contributes a novel DL algorithm for the prediction of a continuous semi-positive structural property and hence defines a regression. Machine Learning (ML) refers to a class of Artificial Intelligence (AI) algorithms that enable systems to learn from a given database and provide new results independently. DL is a subfield of ML that focuses on artificial neural networks (NN) and has been recognized for solving complex engineering and scientific tasks, especially for nonlinear problems. Unlike empirical equations and correlations, ANN models only require sufficient input and output data to be trained. NNs consist of interconnected neurons that use massive parallel computations for identifying the most suitable correlation between inputs and outputs. A neuron is a nonlinear, parameterized (trainable weights and biases *(**w**, b)*) function of input variables, while a NN is a mathematical composition of two or more neurons through an activation function. The nonlinear nature of NNs enables them to identify and model nonlinear behaviors, which may not be captured by other ML methods such as regression techniques. Moreover, NN methods can handle complex, incomplete, and noisy data.

An ML/DL algorithm with parameters *(**w**, b)* is trained through (numerical) minimization of an "error, target, loss, or cost function" $E(\boldsymbol{w}, b)$, where the mean absolute error (MAE), mean squared error (MSE) or its square root (RMSE) is often used for regression problems, which measures the distance between model predictions $\hat{s}$ and obtained training data $s \in D$. It is crucial to split the available data into three subsets: training, validation, and testing data, and ensure that the data in the subsets have a similar distribution for the entire set to guarantee that they are from the same distribution and are representative. Common choices acc. to [28] for the sizes of the amount of data (here $|D| = N_S$ is the number of data points within the whole data set) are: training data: 80% of $|D|$; test data: 10% of $|D|$; validation data: 10% of $|D|$. This approach ensures that the model's performance is evaluated on independent data and that the model does not overfit the training data.

In order to assess the performance and precision of ML/DL models, various validation benchmarks such as RMSE, coefficient of determination R^2, and MAE are typically used. This research focuses on developing an accurate and efficient DL algorithm using artificial neural networks (ANN) to forecast the flexural overstrength factor of steel beams with different cross-sections under pure bending. The proposed DL method also enables the identification of similarities between cross-sections with respect to the flexural overstrength factor by untangling latent correlations within a shared layer, yet we do not employ a specific loss function for measuring encoding quality (e.g. a reconstruction loss) or enforcing a specific probability distribution for the latent variables within the shared layer (e.g. the Kullback-Leibler divergence for variational encoders) of the NN.

4.2 Novel MHER Deep Learning Architecture

This research proposes a novel DL architecture called multi-head encoder - regressor Deep Neural Network (**MHER-DNN**) for twofold use: (i) prediction of the overstrength factor s for five cross section types (CHS, SHS, RHS, I and H) of various steel grades, and (ii) learning a compressed representation of the cross section specific inputs for subsequent regression but also domain-informed inspection. Note, that the MHER-DNN architecture as provided in Fig. 5 is solely used for training as proxy combining the individual models (without the other heads), which have to be used at inference resp. prediction. Inspection of the latent parameters and cross-sectional similarities can be executed on the shared embedding layer.

The MHER-DNN is designed with three input heads, one for each cross-sectional type, i.e. CHS, RHS, SHS, and I

as well as H. The input heads with feature dimensions d_{CHS} = 4, d_{RHSSHS} = 8 and d_{IH} = 9 consist of fully connected Multi-Layer Perceptron (MLP) networks with 'relu' activation function, batch normalisation as well as dropout layers and feed into a shared embedding layer of dimension d_z, which learns the similarities and differences between the cross-section types. The embedding layer output is then passed to the regressor MLP network (also with batch normalisation as well as dropout layers) for predicting the overstrength factor *s* given cross-sectional features for circular, RHS/SHS, and I/H profiles. The MLPs are designed as encoders with decreasing layer width, starting with N_N nodes and a subsequent shrinkage at a rate of $1/N_L$. All MHER-DNN hyperparameters are summarized in Tab. 1.

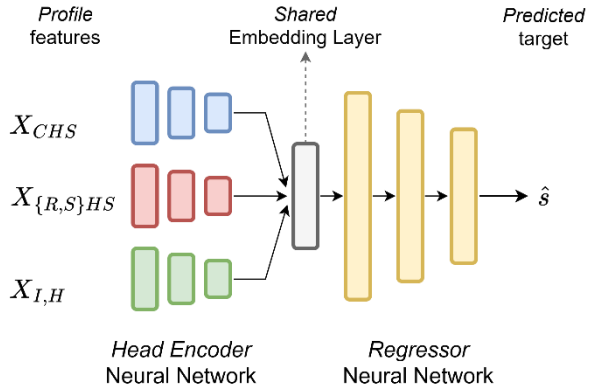

Figure 5 Multi-head encoder – Regressor Deep Neural Network (MHER-DNN) with shared embedding layer for predicting the overstrength factor *s* given cross-sectional features for CHS, RHS, SHS, I and H profiles.

5 Training and Validation of MHER-DNN

The data sets for CHS, RHS, SHS, I and H cross sections are split into training (80% of $N_{S,i}$) set, validation (10% of $N_{S,i}$) set and test (10% of $N_{S,i}$) set. Figs. 2 – 4 proof the respective sub data sets possess approximately similar distributions over the intervals. The data sets were furthermore standardized before training to yield zero mean and unit standard deviation, where a data scaler function per section type was employed and calibrated using the training sets only. Due to the differing sizes of the single cross-sectional data sets within the data base, a custom data loader for consistent batch training was programmed to ensure a fixed batch length during training for the MHER-DNN.

A hyperparameter search was conducted in order to find the MHER-DNN architecture with optimal performance. The hyperparameters investigated are: number of layers N_L, number of nodes N_N nodes, latent space dimension d_z, and dropout rate r_d, while the activation function was not changed. The hyperparameters value ranges spanning the MHER-DNN's search space as well as the final choices are provided in Table 1, where a grid search approach was used to find the optimal combination of hyperparameters.

Each MHER-DNN training run consisted of 2,000 update epochs with 10 training and 5 validation steps per epoch. We employed a MSE loss as objective without further regularization, where the Adam optimizer with initial learning rate of 0.001 is used. The training also enforces callbacks for learning rate reduction and early stopping for tracking the validation loss with patience of 120 respectively 200 epochs. We further utilised the weights&biases framework for automated monitoring, result tracking and reporting of the hyperparameter tuning.

Table 1 DL architecture search space: hyperparameters and ranges for the gridsearch as well as final hyperparameter choices

Hyperparameter	Range	Final Choice
# Layers N_L	[2, 8, 32]	8
# Nodes N_N	[32, 64, 128]	64
Latent Dim d_z	[2, 3, 10, 15]	3
Dropout Rate r_d	[0, 0.25]	0.25

Fig. 6 provides the learning curves of the final MHER-DNN architecture as an example, showing the progress in predictive capabilities. As to be expected, the training losses per section drop over the epochs while the validation losses are slightly higher and thus providing evidence for not overfitting.

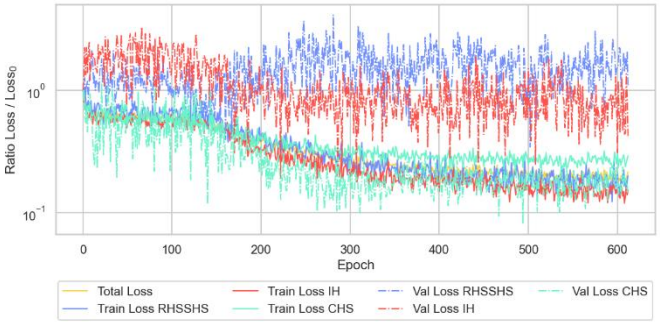

Figure 6 Learning curves: total, training and validation losses for the cross sectional networks per epoch.

A parallel coordinate plot was used in Fig. 7 to visualize the hyperparameters of MHER-DNN as well as the MAE computed by MHER-DNN on the test data sets of the cross sections. The parallel coordinate plot clearly highlights a trade-off between the test set MAEs of the overstrength factor *s* of the three NN models and their hyperparameter choices without a clear favourite choice. Hence the choice of the final MHER-DNN hyperparameters can only be made in a Pareto optimal sense. Therefore we use the average MAE on the test sets (represented by the colorbar in Fig. 7) as decision criterion for choosing the values reported in Tab. 1.

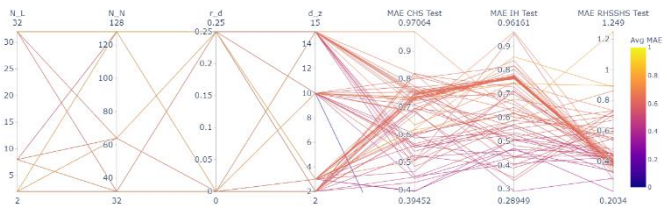

Figure 7 Parallel coordinates plot of the hyperparameter tuning together with the MAE results on the test data sets for the cross sections as well as the average MAE score.

Fig. 8 provides plots for comparing predictions $\hat{s}$ and ground truth data *s* for the finally chosen MHER-DNN hyperparameters for all cross sectional data sets (while different markers indicate training, validation and test data

sets).

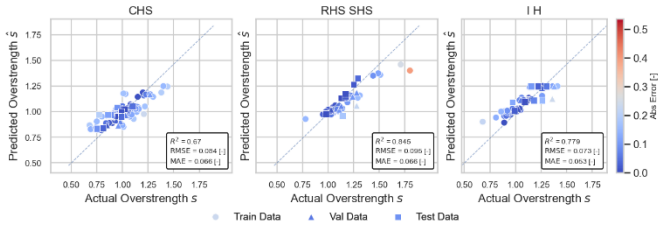

Figure 8 Prediction capability of the MHER-DNN model on the train, validation and test data sets over all cross sections.

First, it should be noted that the three MHER-DNN cross sectional sub-regression models predict their respective targets very well as proven by the respective reported RMSE, MAE and R^2 values. However, approximately linear deviation trends with different magnitudes can be observed. In order to investigate the deviations more closely, Fig. 9 compares the performance of the proposed MHER-DNN models by plotting the overstrength ratios of predictions $\hat{s}$ against the corresponding experimental normalised by the experimental ground truth values s.

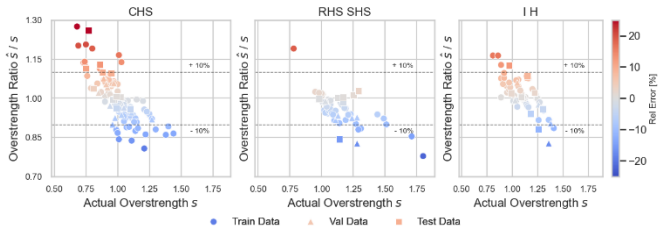

Figure 9 Prediction capability of the MHER-DNN model on the train, validation and test data sets over all cross sections.

In Fig. 9, a normalized value of 1.0 represents a perfect estimation and indicates the most accurate prediction performance area. It can be seen, that most values are within a precision band of +/- 10%, where the linear patterns of predictive deviations confirm model dependent heteroscedasticity. The sub-model deviations manifest in the form that smaller value ranges (on the left side of the diagrams) are generally underestimating overstrength whereas larger value ranges are rather overestimated. The coefficients of variation (CoV) for the cross sectional MHER-DNN sub-models are provided in Tab. 2.

Table 2 Computed Coefficients of Variation (CoV) for the final MHER-DNN on the train, validation and test data sets over all cross sections.

Cross Section	CoV data set	Train set	Val set	Test set
CHS	0.138	0.141	0.106	0.108
RHS SHS	0.146	0.159	0.080	0.079
I H	0.131	0.133	0.119	0.099

A determination of the design values for predictions given by the sub-models together with partial safety factors in accordance with Annex D of EN 1990 is omitted given the brevity of this paper with a reference to [31].

6 Latent Space Inspection and Interpretation

A key feature of the proposed MHER-DNN model is inspection of the cross sectional embeddings into the latent space variables of the shared layer. Latent space inspection is a critical step in evaluating the performance of a deep learning model and gaining understanding of the latent structure within the data. In this regard, the latent space is a low-dimensional representation of the cross sections within the data set learned by the MHER-DNN model during training. As the finally chose MHER-DNN possesses a three dimensional latent space, no further dimensionality reduction e.g. via t-distributed stochastic neighbour embedding (t-SNE) or Uniform Manifold Approximation and Projection (UMAP) projection is necessary for human perception.

Fig. 10 provides a visualisation of the latent space as 3D plot together with projections in the latent dimensions as top and side views. Cross sections are indicated by markers while the colouring highlights the overstrength factor. By examining the visualization in Fig. 10 humans can get a sense of how the MHER-DNN has learned to separate the cross sectional input data together with detection of clusters in the latent representation of the input data.

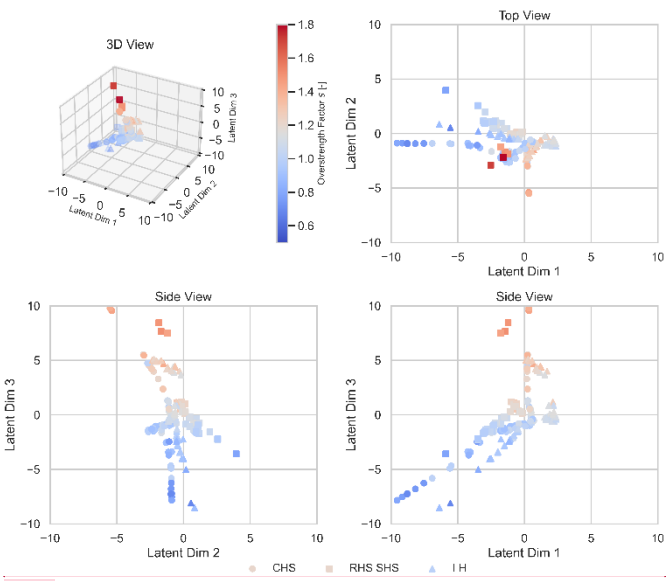

[M1]

Figure 10 Visualisation of the 3-D latent space spanned by the coordinates of the embedding layer of MHER-DNN.

7 Summary, Conclusions and Outlook

This study focuses on addressing the issue of overstrength factor regression for specific types of sections by presenting novel and efficient methods for explicitly formulating relations of cross sectional features with overstrength of steel beams upon five cross section types: CHS, RHS, SHS, I and H. To that end, we propose, train and validate a novel DL architecture called multi-head encoder - regressor Deep Neural Network (MHER-DNN) for twofold use: (i) prediction of the overstrength factor s for the five cross section types, and (ii) learning a compressed representation of the cross section specific inputs for subsequent regression but also domain-informed inspection.

Experimental data for the overstrength factor s of CHS,

RHS, SHS, I and H cross sections containing diverse geometric and material properties furnished as data set. A hyperparameter grid search delivered a moderately sized NN with 3 latent dimension to be best suited for this predictive task. The average RMSE in overstrength for the three submodels is around 8% together with an overall scatter level characterized by a CoV of around 13%, indicating reasonable high precision of the MHER-DNN compared to existing predictive models and for future use in research and engineering practice. We obtained linear yet heteroscedastic deviations of the model predictions with clear over- and underestimation behaviour, where smaller overstrength value ranges are generally overestimated while high values are underestimated.

Another novelty of this paper is the disentanglement of the latent space representation of the MHER-DNN embeddings of the different cross section types w.r.t. overstrength factors, which allows for (i) derivation of common features for prediction of the overstrength factor, and (ii) human inspection and perception of the embeddings. By examining Fig. 10, allows to detect that the model detected several cross sectional clusters in the latent space. The individual clusters seem to possess a 1-dimensional intrinsic dimension (as the data are aligned on one line), however multiple branches within the 3D space can be recognized. Further model architecture changes as well as feature engineering is necessary to further improve the overall model performances due to the obvious intrinsic correlation clusters between the cross sections w.r.t. the overstrength.

Future research is hence concerned with further hyperparameter tuning and model architecture investigations along hybrid autoencoder – multi-head regressor architectures. As the consecutive elaboration of the partial safety factor for the finally chosen DNN prediction model was omitted within this paper, this is a next step in order to establish the trained models as Eurocode-compliant surrogates within the verification process in engineering design practice.

The code for this work is provided online within the github repository of the first author: https://mkrausai.github.io/research/01_SciML/02_Overstrength

References

[1] Mazzolani, F. M., & Piluso, V. (1992, October). Evaluation of the rotation capacity of steel beams and beam-columns. In *Proceedings of 1st State of the Art Workshop COST C* (Vol. 1).

[2] D'Aniello, M.; Landolfo, R.; Piluso, V.; Rizzano, G. (2012) *Ultimate behavior of steel beams under non-uniform bending.* Journal of Constructional Steel Research, 78, 144-158.

[3] Rebelo, C.; Lopes, N.; Da Silva, L. S.; Nethercot, D.; Real, P. V. (2009) *Statistical evaluation of the lateral–torsional buckling resistance of steel I-beams, Part 1: Variability of the Eurocode 3 resistance model.* Journal of Constructional Steel Research, 65(4), 818-831.

[4] da Silva, L. S.; Rebelo, C.; Nethercot, D.; Marques, L.; Simões, R.; Real, P. V. (2009) *Statistical evaluation of the lateral–torsional buckling resistance of steel I-beams, Part 2: Variability of steel properties*. Journal of Constructional Steel Research, 65(4), 832-849.

[5] Sedlacek, G.; Dahl, W.; Stranghöner, N.; Kalinowski, B.; Rondal, J.; Boeraeve, P.H.; (1998) *Investigation of the rotation behaviour of hollow section beams.* European Commission, Technical Steel Research, contract no: 7210-SA/119, final report.

[6] Elchalakani, M.; Zhao, X.L.; Grzebieta, R.H. (2002) *Bending tests to determine slenderness limits for cold-formed circular hollow sections*. Journal of Constructional Steel Research, 58 (11): 1407–30.

[7] Elchalakani M.; Zhao, X.L.; Grzebieta R. H. (2002) Plastic slenderness limit for cold-formed circular hollow sections. Australian Journal of Structural Engineering, 3(3): 127–39.

[8] Jiao, H.; Zhao, X.L. (2004) *Section slenderness limits of very high strength circular steel tubes in bending.* Thin Walled Structures, 42: 1257–71.

[9] Elchalakani, M.; Zhao, X.L.; Grzebieta, R.H. (2004) *Cyclic bending tests to determine fully ductile slenderness limits for cold-formed circular hollow sections.* Journal of Structural Engineering, 127(7): 1001–10.

[10] Kiymaz, G. (2005) *Strength and stability criteria for thin-walled stainless steel circular hollow section members under bending.* Thin-Walled Structures, 43(10), 1534-1549.

[11] Elchalakani, M.; Zhao, X. L.; Grzebieta, R. (2006) *Variable amplitude cyclic pure bending tests to determine fully ductile section slenderness limits for cold-formed CHS*. Engineering Structures, 28(9), 1223-1235.

[12] Haedir, J.; Bambach, M. R.; Zhao, X. L.; Grzebieta, R. H. (2009) *Strength of circular hollow sections (CHS) tubular beams externally reinforced by carbon FRP sheets in pure bending.* Thin-walled structures, 47(10), 1136-1147.

[13] Guo, L.; Yang, S.; Jiao, H. (2013) *Behavior of thin-walled circular hollow section tubes subjected to bending.* Thin-Walled Structures, 73, 281-289.

[14] Wilkinson, T. (1999) *The plastic behaviour of cold formed rectangular hollow sections*. Ph.D. Thesis, Department of Civil Engineering, University of Sydney, Australia.

[15] Zhou, F.; Young, B. (2005) *Tests of cold-formed stainless steel tubular flexural members*. Thin-Walled Structures, 43(9), 1325-1337.

[16] Landolfo, R.; D'Aniello, M.; Brescia, M.; Tortorelli, S. (2011) *Rotation capacity and classification criteria of steel beams.* The development of innovative approaches for the design of steel–concrete structural systems—the line, 5, 2005-2008.

[17] Lukey, A. F.; Adams, P. F. (1969) *Rotation capacity of beams under moment gradient*. Journal of the Structural Division, 95(6), 1173-1188.

[18] Climenhaga, J.J. (1970) *Local buckling in composite beams.* Ph.D. Dissertation, University of Cambridge, Cambridge, England.

[19] Grubb, M. A.; Carskaddan, P. S. (1979) *Autostress design of highway bridges, phase 3: initial moment-rotation tests.* AISI Project, 188, 019-4.

[20] Grubb, M. A.; Carskaddan, P. S. (1981) *Autostress design of highway bridges, phase 3: moment-rotation requirements.* AISI project, 188, 018-1.

[21] Kemp, A. R. (1985) *I interaction of plastic local and lateral buckling.* Journal of Structural Engineering, 111(10), 2181-2196.

[22] Schilling, C. G. (1988) *Moment-rotation tests of steel bridge girders.* Journal of structural Engineering, 114(1), 134-149.

[23] Schilling, C. G. (1990) *Moment-rotation tests of steel girders with ultracompact flanges.* In: Structural Stability Research Council. 1990 Annual Technical Session, Stability of Bridges, St. Louis, Missouri, April 10-11.

[24] Wargsjö, A. (1991) *Plastisk rotationskapacitet hos svetsade stålbalkar* (Doctoral dissertation, Luleå tekniska universitet)

[25] Dahl, W.; Langenberg, P.; Sedlacek, G.; Spangemacher, R. (1992*) Elastisch-plastisches Verhalten von Stahlkonstruktionen- Anforderungen und Werkstoffkennwerte*. Doc.-Nr. 7210-Sa / 118 (91-F6.05), Rheinisch-Westfalischen Technischen Hochshule Aachen, Germany.

[26] Boeraeve, P.; Lognard, B.; Janss, J.; Gerardy, J. C.; Schleich, J. B. (1993) *Elasto-plastic behaviour of steel frame works.* Journal of Constructional Steel Research, 27(1-3), 3-21.

[27] Suzuki, T.; Ogawa, T.; Ikarashi, K. (1994) *A study on local buckling behavior of hybrid beams*. Thin-walled structures, 19(2-4), 337-351.

[28] Frochte, J. (2020) *Maschinelles Lernen - Grundlagen und Algorithmen in Python*. 3. Auflage, München: Carl Hanser Verlag GmbH Co KG, 2019. doi: 10.1091/mbc.E10.

[29] Adeli H,; Yeh C. (1989) *Perceptron learning in engineering design*. Computer- Aided Civil and Infrastructure Engineering, 4, H. 4, S. 247 - 256, doi: 10.1111/j.1467-8667.1989.tb00026.x.

[30] Thai, H.-T. (2022) *Machine learning for structural engineering: A state-of-the-art re-view*, Structures 38, S. 448–491.

[31] Kraus, M. A., Taras, A. (2020) *Physik-informierte Künstliche Intelligenz zur Berechnung und Bemessung im Stahlbau*, Stahlbau 89, H. 10, S. 824 - 832, doi: 10.1002/stab.202000074.

[32] Kraus, M. A., Drass, M. (2020) *Artificial intelligence for structural glass engineering applications - overview, case studies and future potentials*, Glass Structures and Engineering 5, H. 3, S. 247–285, doi: 10.1007/s40940-020-00132-8.

[33] Müller, A., Taras, A., Kraus, M. A. (2022) *Scientific Machine and Deep Learning Investigations of the Local Buckling Behaviour of Hollow Sections*. ce/papers. 5, H. 4, S. 1034 - 1042.

[34] Kraus, M. A. (2022) *Erklärbare domänenspezifische Künstliche Intelligenz im Massiv- und Brückenbau*, Beton- und Stahlbetonbau 117, H. 10, S. 795 - 804, doi: 10.1002/best.202200079.

[35] Kraus, M. A. et al. (2022) *Künstliche Intelligenz – multiskale und cross-domäne Synergien von Raumfahrt und Bauwesen* in: Bergmeister, K.; Fingerloos, F.; Wörner, J.-D. [Hrsg.] Beton-Kalender 2022. Berlin: Ernst & Sohn, S. 607-690.

[36] D'Aniello, M.; Güneyisi, E. M.; Landolfo, R.; Mermerdaş, K. (2014) *Analytical prediction of available rotation capacity of cold-formed rectangular and square hollow section beams.* Thin-Walled Structures, H. 77, pp. 141-152.

[37] Guzelbey, I. H.; Cevik, A.; Gögüş, M. T. (2006) *Prediction of rotation capacity of wide flange beams using neural networks.* Journal of Constructional Steel Research 62, H. 10, pp. 950-961.

[38] D'Aniello, M.; Güneyisi, E. M.; Landolfo, R.; Mermerdaş, K. (2015) *Predictive models of the flexural overstrength factor for steel thin-walled circular hollow section beams*. Thin-Walled Structures, H. 94, pp. 67-78

[39] Müller, A.; Taras, A. (2022) *Prediction of the load-displacement and local buckling behavior of hollow structural sections using Deep Neural Networks (DNN).* Proceeding of SSRC, Denver.

[40] Müller, A.; Taras, A. (2022) *Prediction of the local buckling strength and load-displacement behaviour of SHS and RHS members using Deep Neural Networks (DNN). Introduction to the Deep Neural Network Direct Stiffness Method (DNN-DSM).* Steel Construction 15, Hollow Sections, pp. 78-90.

[41] Müller, A.; Taras, A.; Kraus, A.K. (2022) *Scientific Machine Learning and Deep Learning Investigations of the Local Buckling Behaviour of Hollow Sections.* Proceedings of SDSS, Aveiro, Portugal.

[42] Müller, A.; Taras, A. (2023) Prediction of the deformation and local buckling behavior of structural systems using the deep neural network direct stiffness method (DNN-DSM). Proceedings of the Annual Stability Conference Structural Stability Research Council (SSRC), Charlotte, North Carolina.